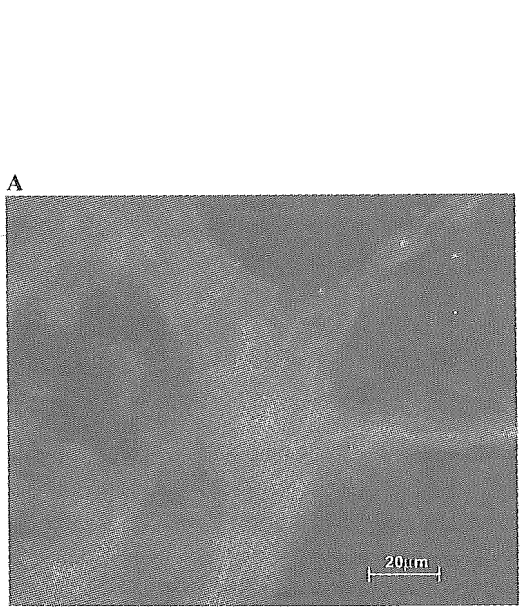

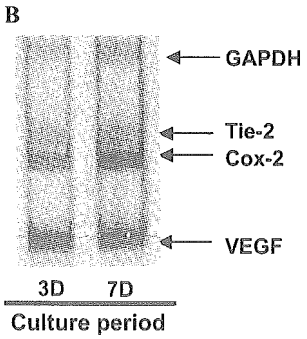

C

Gene	Result
VEGF	++
Cox-2	++
Tie-2	++
Ang-1	+
Ang-2	-

Fig. 1. Cardiac cell sheets have intrinsic angiogenic potential. (A) Endothelial cells within cardiac cell sheets were detected as CD31-expressing cells (green). Nuclei (blue) are counterstained with Hoechst 33342. (B) RT-PCR analysis of RNA isolated from cardiac cell sheets shows positive expression for VEGF, Cox-2, and Tie-2 at both 3 and 7 days in culture. (C) Total gene expression analysis of angiogenesis-related genes detected in cardiac cell sheets by RT-PCR. (++) indicates expression, (+) indicates occasional expression, and (−) indicates no expression.

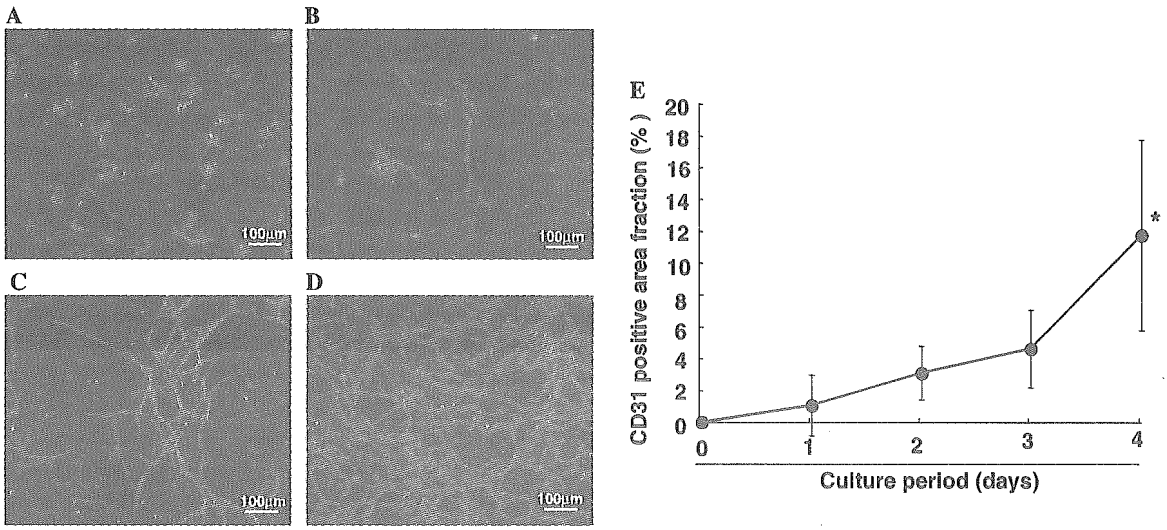

Fig. 2. Endothelial cells within cardiac cell sheets grow in a sprouting fashion. CD31 expression within the cardiac cell sheets was detected at (A) 1 day, (B) 2 days, (C) 3 days, and (D) 4 days, in culture. (E) The graph shows the percentage of CD31-positive areas of the myocardial cell sheets at each time period. ($*p < 0.05$, $n = 3$).

Neovascularization of myocardial tissue grafts occurs upon in vivo transplantation

To determine the origin of newly formed blood vessels within the myocardial tissue grafts in vivo, we stacked three cardiac cell sheets derived from EGFP-expressing neonatal rats and transplanted these triple-layer grafts into the dorsal subcutaneous tissues of normal rats. When the transplantation sites were opened 1 week after the procedures, the implanted grafts showed synchronous and spontaneous pulsation and maintained their original shapes, indicating whole tissue survival. Upon histological analysis

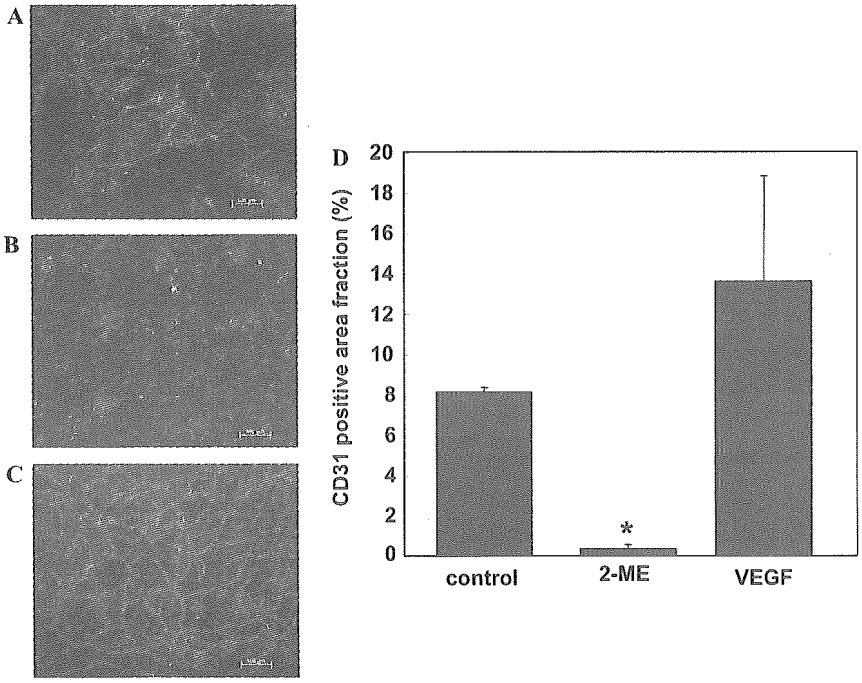

Fig. 3. Endothelial cells within cardiac cell sheets are reactive. Immunostaining for CD31 in (A) control, (B) cells treated with 2 μM 2-methoxyestradiol or (C) 10 nM rat recombinant VEGF shows changes in endothelial cell network formation after 4 days in culture. (D) The graph shows the percentage of CD31-positive areas of the myocardial cell sheets treated under each condition ($*p < 0.05$, $n = 3$).

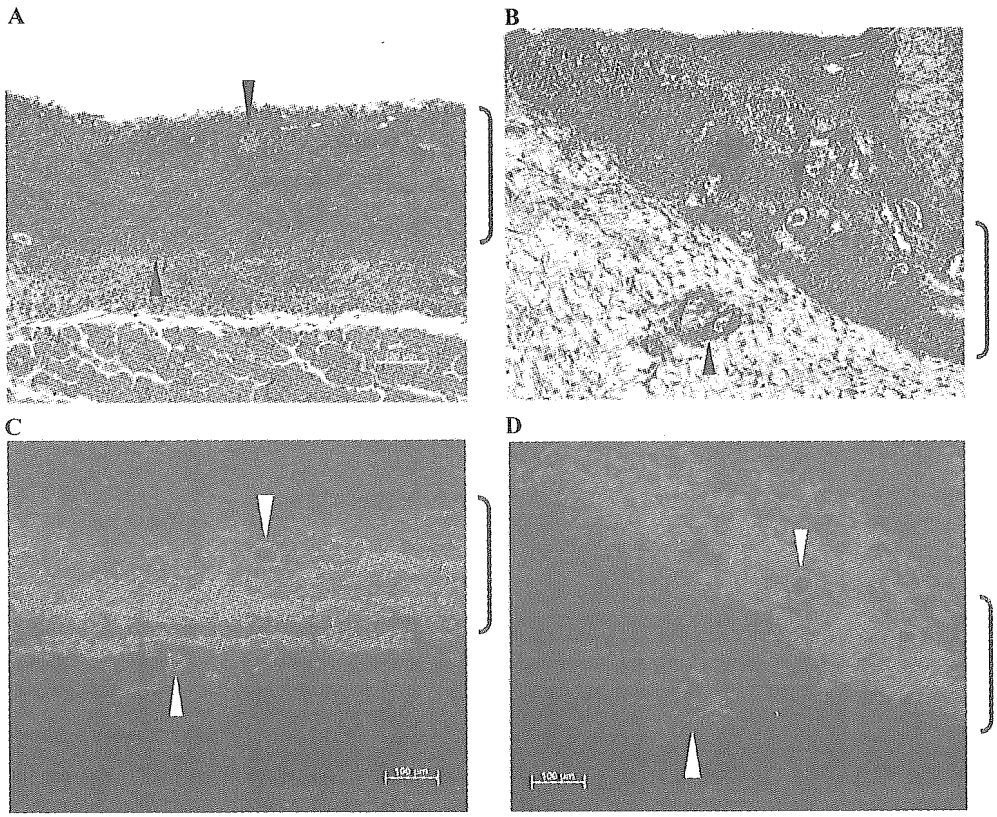

Fig. 4. Microvessel formation within transplanted triple-layer cardiac cell sheets. One week after transplantation, (A,B) show hematoxylin and eosin staining which shows the formation of microvessels containing host erythrocytes within the transplanted grafts and in the underlying host tissues (black arrowheads). (C,D) Anti-EGFP immunostaining (red fluorescence) identifies graft-derived cells. Arrows indicate that the vessels observed in (A,B) are EGFP-positive and contain host erythrocytes within the lumen of the vessels (white arrowheads). Note that EGFP-positive vessels sprout into the host tissue.

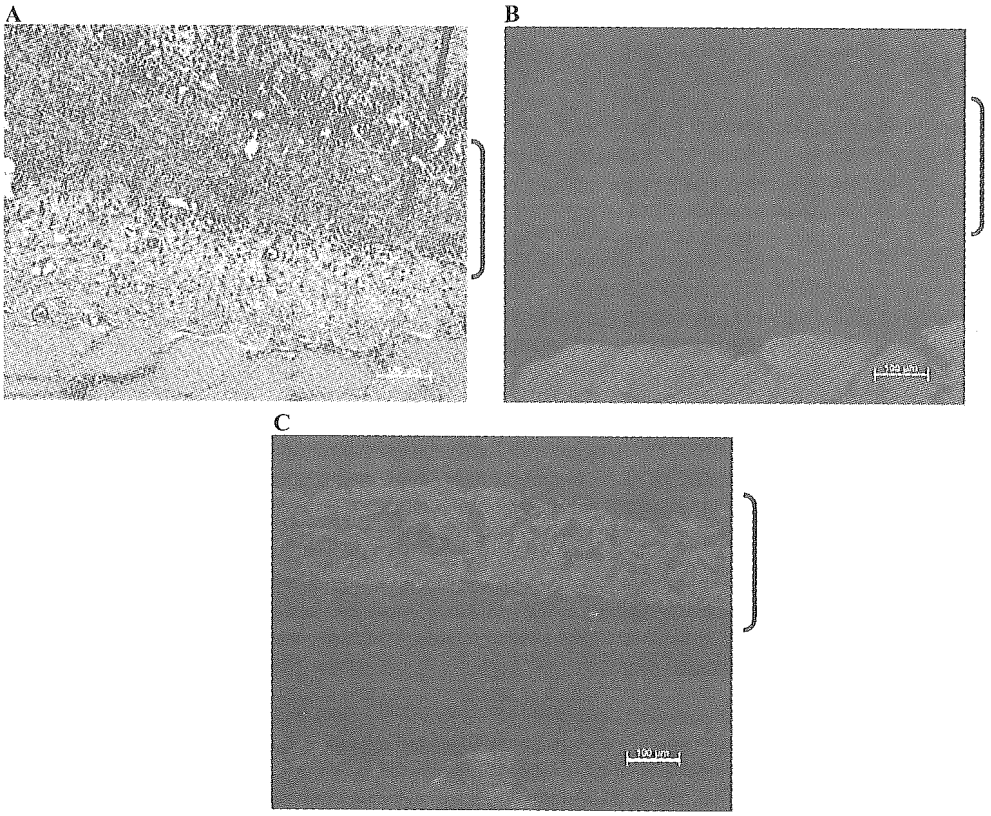

Fig. 5. Immunohistological analysis of the myocardial tissue grafts transplanted subcutaneously into EGFP-expressing host rats. One week after transplantation, (A) hematoxylin and eosin staining demonstrates microvessel formation within the EGFP-negative transplanted tissues. (B) Immunostaining for EGFP (red) shows almost no positive staining within the transplanted grafts, indicating that the vessel formation is due to EGFP-negative graft cells. (C) anti-α-sarcomeric actinin demonstrates the presence of cardiac muscle in the transplanted grafts.

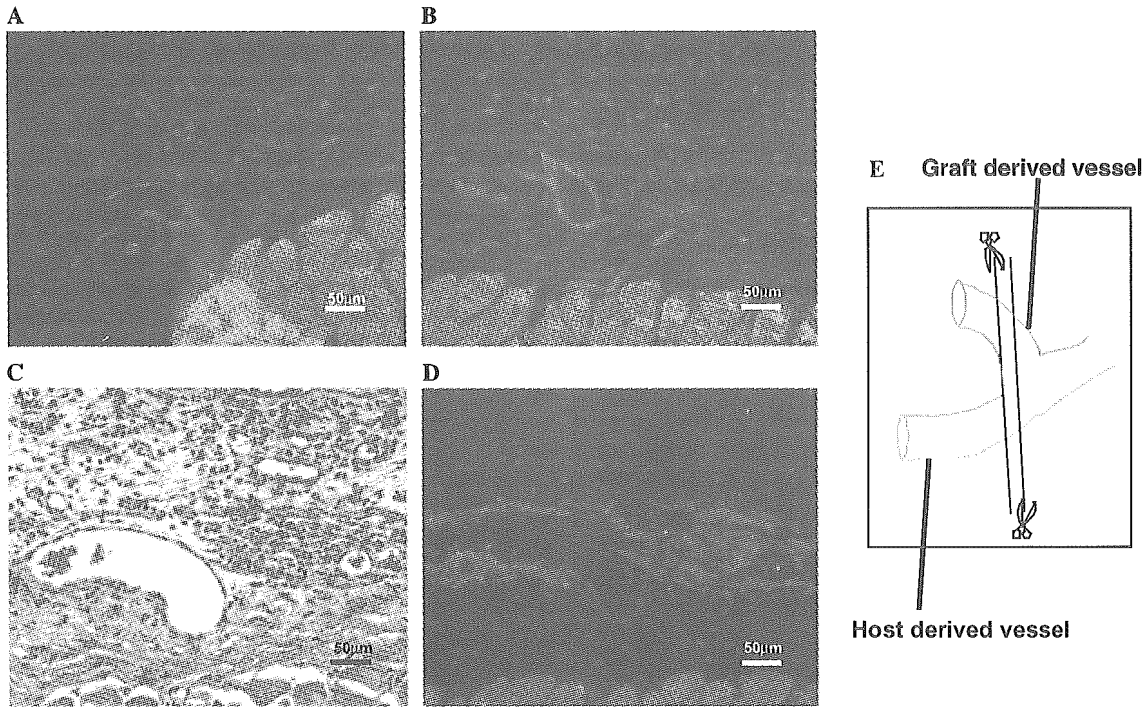

Fig. 6. Fused vessels at the junction between the EGFP-expressing host tissues and the transplanted grafts. (A,B) Immunostaining EGFP (green) demonstrates that EGFP-negative graft endothelial cells fuse with EGFP-positive host cells to form mature microvessels. (C) Hematoxylin and eosin staining of a serial section to (A,B) shows erythrocytes within the vessel lumen. (D) Immunostaining for α-sarcomeric actinin (green) shows that the vessel is at the border between the transplanted cardiac grafts and the underlying host tissues. (E) Presents a schematic illustration of the observed serial sections.

of resected tissues, well-established vascular structures within the grafts were observed, similar to our previously reported results [21] (Figs. 4A and B). Unexpectedly however, anti-GFP antibody staining clearly demonstrated that almost all blood vessels in the grafts expressed EGFP and were therefore graft-derived (Figs. 4C and D). Furthermore, some EGFP-expressing blood vessels, originating from the transplanted grafts, could even be detected within the host tissues just beneath the implanted cardiac tissues (Figs. 4C and D).

To determine whether host-derived vessels migrated into the transplanted cardiac grafts, EGFP-negative myocardial tissue grafts were transplanted into EGFP-expressing host rats. One week after transplantation, no EGFP-positive blood vessels could be detected within the myocardial tissue grafts (Figs. 5A and B), which were positively stained for cardiac muscle, by anti-α-sarcomeric actinin antibody (Fig. 5C). Using staining of serial cross-sections, it was also observed that EGFP-positive host vessels fused with EGFP-negative graft vessels at the border region between the transplanted myocardial grafts and the underlying host subcutaneous tissues (Fig. 6). These results therefore indicated that endothelial cell networks within the cell sheets mature to form tubularized vascular networks within the grafts after in vivo transplantation. Additionally, these newly formed vessels that originated completely from the grafts migrated into the underlying tissues to connect with host blood vessels.

Controlling neovascularization within myocardial tissue grafts

Due to the observation that the newly formed vessels within the implanted myocardial tissues were completely graft-derived, we tried to control the ratio of endothelial cells within the fabricated cardiac cell sheets and exam-

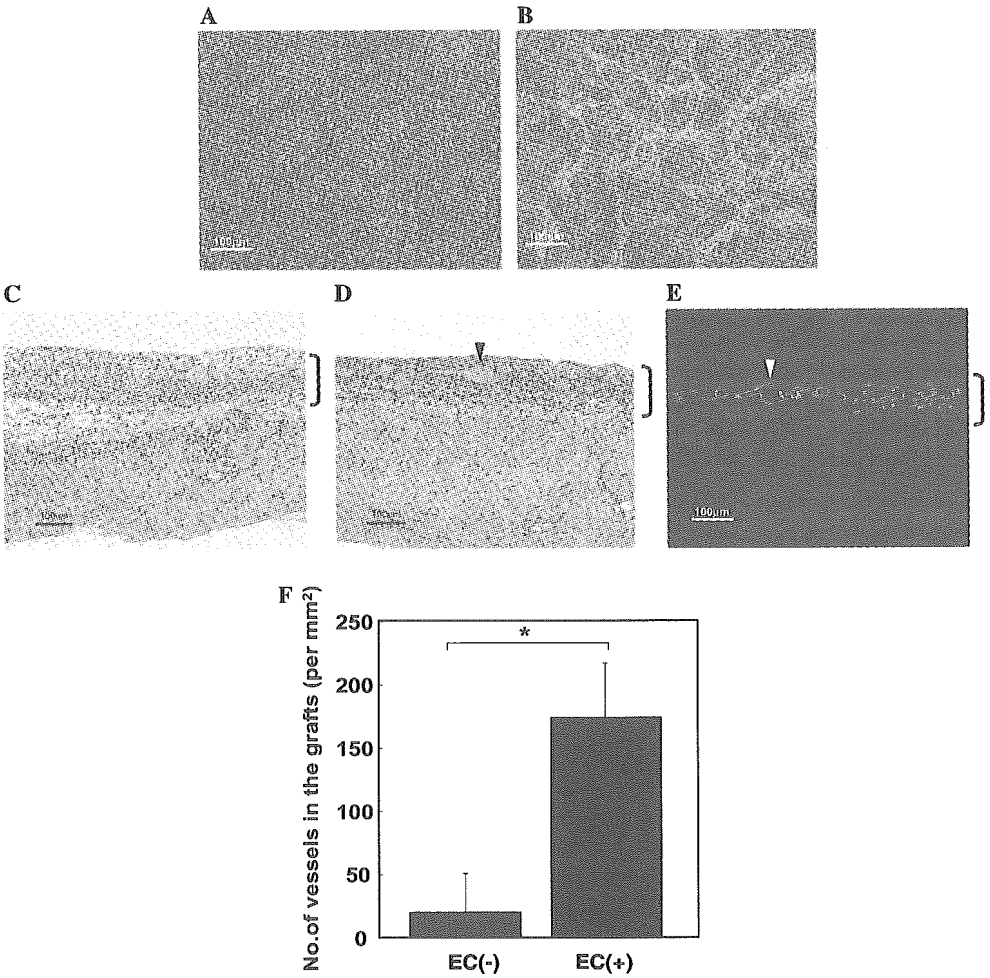

Fig. 7. Control of endothelial cells allows for the regulation of in vivo neovascularization. Endothelial cells were removed from isolated cardiac cell suspensions by MACS. (A) Anti-CD31 staining shows that cardiac cell suspensions without endothelial cells do not form sprouting endothelial cell networks in vitro. (B) When endothelial cells were added to cardiac cells at a ratio of 1:9, in vitro sprouting network formation could be recovered. (C) Three days after triple-layer subcutaneous transplantation, cardiac cell sheets with no endothelial cells demonstrate no vessel formation in vivo. (D) In contrast, when EGFP-positive endothelial cells were added at a ratio of 1:9, in vivo blood vessel formation was also recovered. (E) Anti-EGFP immunostaining demonstrates that all the blood vessels within the grafts are derived from graft-originating EGFP-positive cells (green). (F) Quantitative analysis of vessel formation within the fabricated grafts is presented. EC (−) indicates the grafts fabricated without endothelial cells and EC (+) created with endothelial cells and cardiac cells at a ratio of 1:9. ($*p < 0.05$, $n = 3$).

ined the effect on graft neovascularization in vivo. Endothelial cells were separated from primary isolated cardiac cell suspensions by MACS and accounted for $18.9 \pm 9.8\%$ ($n = 7$) of the total isolated cell suspensions. When cardiac cell sheets without endothelial cells were fabricated from the remaining cell suspensions after MACS, significantly fewer endothelial networks were observed (Fig. 7A). However, when endothelial cell-depleted cardiac cells were mixed with EGFP-positive endothelial cells at a ratio of 9:1, the previously observed endothelial cell networks could be completely recovered within these hybrid cell sheets (Fig. 7B). Upon subcutaneous transplantation of triple-layer mixed cell sheets into nude rats, graft-originated EGFP-positive blood vessels were clearly observed within the transplanted myocardial tissue grafts (Figs. 7D and E). When transplanted grafts were composed of cell sheets without endothelial cells, a significantly lower amount of blood vessels were observed 3 days after implantation (Fig. 7C), compared to the hybrid cell sheet group that contained a controlled ratio of endothelial cells. These findings therefore confirmed that the endothelial cells within the cell sheet grafts contribute significantly to the formation of new blood vessels within the bioengineered tissues (Fig. 7F). Moreover, by controlling the ratio of endothelial cells initially seeded in the cardiac cell sheets, neovascularization of the fabricated grafts could also be regulated.

Discussion

There have been several previous studies regarding micro blood vessel formation of tissue implants without surgical vascular anastomoses. When human skin grafts were transplanted onto athymic mice, graft vessels became anastomosed to the host circulation, but over time, human endothelial cells from the transplanted grafts progressively degenerate while host endothelial cells invade to gradually replace the graft-derived cells [23]. Similarly, in the case of pancreatic islet grafts transplanted both subcutaneously and to the kidney capsule, the transplanted tissues were shown to be mainly re-vascularized by endothelial cells of host origin [24,25]. Additionally, when cultured skin substitutes were transplanted into rat subcutaneous tissues, new blood vessel formation was shown to be due to both graft- and host-derived endothelial cells [26].

In contrast to these previously reported results, when we transplanted triple-layer cardiac cell sheet constructs into dorsal subcutaneous tissues, the observed blood vessel reconstruction was completely due to the endothelial cell networks that originated from within the grafts. Interestingly, these newly formed graft-derived blood vessels also sprouted into the underlying host tissues, to form functional connections with the host vasculature. Furthermore, vasculature regulation experiments in vivo also demonstrated that the endothelial cell network in vitro forms functional microvessels and sprout into the host tissues after transplantation.

Many biological factors, such as ECM molecules and secreted proteins, have been shown to be important for endothelial cell network formation in engineered tissues [27]. It is well known that when endothelial cells are cultured in three-dimensional Matri-gel and collagen-based gels, they undergo a reversible transition from a resting cobblestone formation to a sprouting angiogenic phenotype [28,29]. Similarly, when endothelial cells were included in the cardiac cell sheets, they showed this sprouting form and network development in vitro, even though additional ECM substitutes were not used. With our method, the isolated cell suspensions include not only cardiomyocytes and endothelial cells, but also a significant number of fibroblasts and other ECM-producing cells. Therefore, it is likely that these cells can produce the appropriate ECM molecules such as collagen, which can act to promote endothelial network formation within the cardiac cell sheets.

In combination with the ECM environment, various secreted proteins, such as growth factors and cytokines, have also been shown to be involved in the neovascularization processes. In our results, mRNA expression of both VEGF and Cox-2 was observed, in vitro within the cardiac cell sheets. It has been reported that VEGF secretion via cardiomyocytes is required for the development of coronary microvessels [30], and VEGF gene expression of cultured cardiomyocytes has been also previously demonstrated [31]. Cox-2 is also a key enzyme involved in angiogenesis and known to be expressed in cardiomyocytes [32]. Furthermore, when human umbilical vein endothelial cells were cultured with conditioned medium derived from rat neonatal cardiomyocytes, Cox-2 expression was also induced in the endothelial cells by VEGF secreted by the cardiac cells [33], indicating that VEGF production by cardiomyocytes within the cell sheets, and Cox-2 expression, may accelerate endothelial sprouting and network formation. Likewise, direct cell-to-cell interactions between cardiomyocytes and endothelial cells have been reported to rescue cardiomyocytes from undergoing apoptosis in vitro, with these effects enhanced compared to the use of conditioned media [34]. Previously, the co-culture of endothelial cells, fibroblasts, and skeletal myoblasts, within three-dimensional porous scaffolds, has also shown to play a significant role in the vascularization of engineered skeletal muscle [27], demonstrating the importance of cell-to-cell interactions in creating endothelial cell networks. In cardiac cell sheets, the observation that cardiomyocyte clusters surround areas enriched with endothelial cells also suggests that the endothelial cell networks are activated by both direct cell-to-cell interactions, as well as secreted proteins from cardiomyocytes. Therefore, a mutually beneficial relationship between cardiomyocytes and endothelial cells seems to contribute to the formation of endothelial cell networks in vitro.

A key factor in the ability for the rapid neovascularization of the bioengineered grafts in vivo is the use of cell sheet engineering with temperature-responsive culture dishes, which are created by the covalent grafting of the

temperature-responsive polymer, PIPAAm, onto ordinary tissue culture polystyrene (TCPS) surfaces [13,19]. With traditional cell harvest methods using proteolytic enzymes such as trypsin, cells are collected as single or isolated cell suspensions. In such cases, it can be expected that the endothelial networks that have been formed, as well as crucial cell-to-cell interactions between cardiomyocytes and endothelial cells, would be disrupted. With temperature-responsive dishes, cells can be cultured on these surfaces similarly onto normal TCPS surfaces at 37 °C. However, by simply reducing the culture temperature to 20 °C, the dish surfaces undergo a reversible transition from hydrophobic to hydrophilic. When this occurs, the grafted polymer rapidly swells, such that a hydration layer is formed between the dish surface and the cultured cells, allowing for all the cultured cells along with their deposited ECM to be non-invasively harvested as intact sheets [20]. Therefore, with cardiac cell sheets harvested from temperature-responsive dishes, their own deposited ECM is preserved, and the cell sheets are also able to retain intact, undisrupted endothelial cell networks, as well as the expression of angiogenesis-accelerating genes such as VEGF and Cox-2. The ability to maintain the differentiated state that has developed during culture is in stark contrast to cell harvest with proteolytic enzymes and allows for the rapid development of graft-derived endothelial cell networks into mature microvessels upon transplantation of these bioengineered tissues with an innate ability for vascularization.

For future applications of tissue engineering, and more specifically related to cardiac tissues, the creation of thick, cell-dense constructs with functional vessels is required. Yet at the present time, growth factor administration and gene therapies methods still remain relatively difficult to control both in vitro and in vivo. In the present study however, upon determining the neovascularization mechanisms of myocardial tissue grafts, we clearly demonstrate the possibility of controlling in vivo vascularization by regulating the ratio of endothelial cells in cardiomyocyte sheets. From these results, it is clearly conceivable that by applying the co-culture of different endothelial cell sources and varying the ratio of endothelial cells within the grafts, optimal conditions for blood vessel fabrication within specific tissues can be created.

Similarly, while the formation of endothelial cell networks can be controlled, these immature networks can survive for only 1 week, in vitro (data not shown). Therefore, not only biological factors but also physical stimuli such as flow and shear stress are likely required to mimic the in vivo environment and allow for the formation of mature vascular networks, under in vitro conditions [35,36].

In conclusion, myocardial tissue grafts engineered with cell sheet technology have their own inherent potential for the in vivo reconstruction of blood vessels. By controlling the endothelial cell population within the cardiac cell sheets, the potential for vascularization can also be regulated, which will likely overcome the limits of mass transport to create thick and functional tissues. This engineering of structures that more closely resemble native tissues has the potential for new applications for tissue engineering and regenerative medicine, as well as other areas, by creating more realistic experimental model systems.

Acknowledgments

We appreciate the useful comments and technical criticism from Mr. Joseph Yang (Tokyo Women's Medical University). We also thank Prof. Masaru Okabe (Osaka University) for kindly providing EGFP transgenic rats and Ms. Yuko Kanauchi (Toho University) for helpful assistance with the endothelial cell regulation studies. The present work was supported by grants for the Center of Excellence Program for the 21st Century, the High-Tech Research Center Program and Grant-in Aid for Young Scientists (B) from the Ministry of Education, Culture, Sports, Science and Technology (MEXT); the Research Grants for Cardiovascular Disease and Regenerative Medicine from the Ministry of Health, Labour and Welfare; and the Open Research Grant from the Japanese Research Promotion Society for Cardiovascular Diseases.

References

[1] W. Risau, Mechanisms of angiogenesis, Nature 386 (1997) 671–674.
[2] W. Risau, I. Flamme, Vasculogenesis, Annu. Rev. Cell Dev. Biol. 11 (1995) 73–91.
[3] J. Folkman, Angiogenesis in cancer, vascular, rheumatoid and other disease, Nat. Med. 1 (1995) 27–31.
[4] M. Ueda, Y. Terai, K. Kanda, M. Kanemura, M. Takehara, H. Futakuchi, H. Yamaguchi, M. Yasuda, K. Nishiyama, M. Ueki, Tumor angiogenesis and molecular target therapy in ovarian carcinomas, Hum. Cell 18 (2005) 1–16.
[5] A. Kawamoto, H.C. Gwon, H. Iwaguro, J.I. Yamaguchi, S. Uchida, H. Masuda, M. Silver, H. Ma, M. Kearney, J.M. Isner, T. Asahara, Therapeutic potential of ex vivo expanded endothelial progenitor cells for myocardial ischemia, Circulation 103 (2001) 634–637.
[6] C.J. Koh, A. Atala, Tissue engineering, stem cells, and cloning: opportunities for regenerative medicine, J. Am. Soc. Nephrol. 15 (2004) 1113–1125.
[7] K.M. Kulig, J.P. Vacanti, Hepatic tissue engineering, Transpl. Immunol. 12 (2004) 303–310.
[8] H.M. Nugent, E.R. Edelman, Tissue engineering therapy for cardiovascular disease, Circ. Res. 92 (2003) 1068–1078.
[9] M. Brittberg, A. Lindahl, A. Nilsson, C. Ohlsson, O. Isaksson, L. Peterson, Treatment of deep cartilage defects in the knee with autologous chondrocyte transplantation, N. Engl. J. Med. 331 (1994) 889–895.
[10] R.S. Kirsner, V. Falanga, W.H. Eaglstein, The development of bioengineered skin, Trends Biotechnol. 16 (1998) 246–249.
[11] T. Shin'oka, Y. Imai, Y. Ikada, Transplantation of a tissue-engineered pulmonary artery, N. Engl. J. Med. 344 (2001) 532–533.
[12] T. Walles, T. Herden, A. Haverich, H. Mertsching, Influence of scaffold thickness and scaffold composition on bioartificial graft survival, Biomaterials 24 (2003) 1233–1239.
[13] N. Yamada, T. Okano, H. Sakai, F. Karikusa, Y. Sawasaki, Y. Sakurai, Thermo-responsive polymeric surfaces; control of attachment and detachment of cultured cells, Makromol. Chem. Rapid Commun. 11 (1990) 571–576.
[14] M. Harimoto, M. Yamato, M. Hirose, C. Takahashi, Y. Isoi, A. Kikuchi, T. Okano, Novel approach for achieving double-layered cell sheets co-culture: overlaying endothelial cell sheets onto monolayer

hepatocytes utilizing temperature-responsive culture dishes, J. Biomed. Mater. Res. 62 (2002) 464–470.
[15] K. Nishida, M. Yamato, Y. Hayashida, K. Watanabe, N. Maeda, H. Watanabe, K. Yamamoto, S. Nagai, A. Kikuchi, Y. Tano, T. Okano, Functional bioengineered corneal epithelial sheet grafts from corneal stem cells expanded ex vivo on a temperature-responsive cell culture surface, Transplantation 77 (2004) 379–385.
[16] K. Nishida, M. Yamato, Y. Hayashida, K. Watanabe, K. Yamamoto, E. Adachi, S. Nagai, A. Kikuchi, N. Maeda, H. Watanabe, T. Okano, Y. Tano, Corneal reconstruction with tissue-engineered cell sheets composed of autologous oral mucosal epithelium, N. Engl. J. Med. 351 (2004) 1187–1196.
[17] Y. Shiroyanagi, M. Yamato, Y. Yamazaki, H. Toma, T. Okano, Urothelium regeneration using viable cultured urothelial cell sheets grafted on demucosalized gastric flaps, BJU Int. 93 (2004) 1069–1075.
[18] J. Yang, M. Yamato, C. Kohno, A. Nishimoto, H. Sekine, F. Fukai, T. Okano, Cell sheet engineering: recreating tissues without biodegradable scaffolds, Biomaterials 26 (2005) 6415–6422.
[19] T. Okano, N. Yamada, H. Sakai, Y. Sakurai, A novel recovery system for cultured cells using plasma-treated polystyrene dishes grafted with poly(*N*-isopropylacrylamide), J. Biomed. Mater. Res. 27 (1993) 1243–1251.
[20] A. Kushida, M. Yamato, C. Konno, A. Kikuchi, Y. Sakurai, T. Okano, Decrease in culture temperature releases monolayer endothelial cell sheets together with deposited fibronectin matrix from temperature-responsive culture surfaces, J. Biomed. Mater. Res. 45 (1999) 355–362.
[21] T. Shimizu, M. Yamato, Y. Isoi, T. Akutsu, T. Setomaru, K. Abe, A. Kikuchi, M. Umezu, T. Okano, Fabrication of pulsatile cardiac tissue grafts using a novel 3-dimensional cell sheet manipulation technique and temperature-responsive cell culture surfaces, Circ. Res. 90 (2002) e40–e48.
[22] M. Hirose, O.H. Kwon, M. Yamato, A. Kikuchi, T. Okano, Creation of designed shape cell sheets that are noninvasively harvested and moved onto another surface, Biomacromolecules 1 (2000) 377–381.
[23] M. Demarchez, D.J. Hartmann, M. Prunieras, An immunohistological study of the revascularization process in human skin transplanted onto the nude mouse, Transplantation 43 (1987) 896–903.
[24] T. Linn, K. Schneider, H.P. Hammes, K.T. Preissner, H. Brandhorst, E. Morgenstern, F. Kiefer, R.G. Bretzel, Angiogenic capacity of endothelial cells in islets of Langerhans, FASEB J. 17 (2003) 881–883.
[25] P. Vajkoczy, A.M. Olofsson, H.A. Lehr, R. Leiderer, F. Hammersen, K.E. Arfors, M.D. Menger, Histogenesis and ultrastructure of pancreatic islet graft microvasculature. Evidence for graft revascularization by endothelial cells of host origin, Am. J. Pathol. 146 (1995) 1397–1405.
[26] D.M. Supp, K. Wilson-Landy, S.T. Boyce, Human dermal microvascular endothelial cells form vascular analogs in cultured skin substitutes after grafting to athymic mice, FASEB J. 16 (2002) 797–804.
[27] S. Levenberg, J. Rouwkema, M. Macdonald, E.S. Garfein, D.S. Kohane, D.C. Darland, R. Marini, C.A. van Blitterswijk, R.C. Mulligan, P.A. D'Amore, R. Langer, Engineering vascularized skeletal muscle tissue, Nat. Biotechnol. 23 (2005) 879–884.
[28] S. Kobayashi, E. Ito, R. Honma, Y. Nojima, M. Shibuya, S. Watanabe, Y. Maru, Dynamic regulation of gene expression by the Flt-1 kinase and Matrigel in endothelial tubulogenesis, Genomics 84 (2004) 185–192.
[29] I. Segura, A. Serrano, G.G. De Buitrago, M.A. Gonzalez, J.L. Abad, C. Claveria, L. Gomez, A. Bernad, A.C. Martinez, H.H. Riese, Inhibition of programmed cell death impairs in vitro vascular-like structure formation and reduces in vivo angiogenesis, FASEB J. 16 (2002) 833–841.
[30] F.J. Giordano, H.P. Gerber, S.P. Williams, N. VanBruggen, S. Bunting, P. Ruiz-Lozano, Y. Gu, A.K. Nath, Y. Huang, R. Hickey, N. Dalton, K.L. Peterson, J. Ross Jr., K.R. Chien, N. Ferrara, A cardiac myocyte vascular endothelial growth factor paracrine pathway is required to maintain cardiac function, Proc. Natl. Acad. Sci. USA 98 (2001) 5780–5785.
[31] A.P. Levy, N.S. Levy, J. Loscalzo, A. Calderone, N. Takahashi, K.T. Yeo, G. Koren, W.S. Colucci, M.A. Goldberg, Regulation of vascular endothelial growth factor in cardiac myocytes, Circ. Res. 76 (1995) 758–766.
[32] N. Degousee, J. Martindale, E. Stefanski, M. Cieslak, T.F. Lindsay, J.E. Fish, P.A. Marsden, D.J. Thuerauf, C.C. Glembotski, B.B. Rubin, MAP kinase 6-p38 MAP kinase signaling cascade regulates cyclooxygenase-2 expression in cardiac myocytes in vitro and in vivo, Circ. Res. 92 (2003) 757–764.
[33] G. Wu, A.P. Mannam, J. Wu, S. Kirbis, J.L. Shie, C. Chen, R.J. Laham, F.W. Sellke, J. Li, Hypoxia induces myocyte-dependent COX-2 regulation in endothelial cells: role of VEGF, Am. J. Physiol. Heart Circ. Physiol. 285 (2003) H2420–H2429.
[34] D.A. Narmoneva, R. Vukmirovic, M.E. Davis, R.D. Kamm, R.T. Lee, Endothelial cells promote cardiac myocyte survival and spatial reorganization: implications for cardiac regeneration, Circulation 110 (2004) 962–968.
[35] B.P. Chen, Y.S. Li, Y. Zhao, K.D. Chen, S. Li, J. Lao, S. Yuan, J.Y. Shyy, S. Chien, DNA microarray analysis of gene expression in endothelial cells in response to 24-h shear stress, Physiol. Genomics 7 (2001) 55–63.
[36] J.P. Cullen, S. Sayeed, R.S. Sawai, N.G. Theodorakis, P.A. Cahill, J.V. Sitzmann, E.M. Redmond, Pulsatile flow-induced angiogenesis: role of G(i) subunits, Arterioscler. Thromb. Vasc. Biol. 22 (2002) 1610–1616.

nature biotechnology

Transient inhibition of BMP signaling by Noggin induces cardiomyocyte differentiation of mouse embryonic stem cells

Shinsuke Yuasa[1,2], Yuji Itabashi[1], Uichi Koshimizu[4], Tomofumi Tanaka[4], Keijiro Sugimura[4], Masayoshi Kinoshita[1], Fumiyuki Hattori[2,4], Shin-ichi Fukami[3], Takuya Shimazaki[3], Hideyuki Okano[3,5], Satoshi Ogawa[1] & Keiichi Fukuda[2]

Embryonic stem (ES) cells are a promising source of cardiomyocytes, but clinical application of ES cells has been hindered by the lack of reliable selective differentiation methods. Differentiation into any lineage is partly dependent on the regulatory mechanisms of normal early development. Although several signals, including bone morphogenetic protein (BMP)[1,2], Wnt[3] and FGF[4], are involved in heart development, scarce evidence is available about the exact signals that mediate cardiomyocyte differentiation. While investigating the involvement of BMP signaling in early heart formation in the mouse, we found that the BMP antagonist Noggin is transiently but strongly expressed in the heart-forming region during gastrulation and acts at the level of induction of mesendoderm to establish conditions conducive to cardiogenesis. We applied this finding to develop an effective protocol for obtaining cardiomyocytes from mouse ES cells by inhibition of BMP signaling.

BMP signaling is crucial in mesodermal induction and cardiac formation[1,2]. However, simple stimulation with BMP2/BMP4 did not augment or suppress cardiomyocyte induction from ES cells (data not shown). In the vertebrate nervous system, Noggin and other BMP inhibitors (chordin and follistatin) are involved in neural differentiation in a context-dependent fashion[5,6]. We hypothesized that BMP antagonists may also be involved in cardiomyocyte induction. Here, we performed whole-mount *in situ* hybridization for various BMP antagonists on mouse embryos at different gastrulation stages. The BMP antagonist Noggin was transiently but strongly expressed in the heart-forming area (**Fig. 1a,b**). It was clearly expressed at the cardiac crescent at mouse embryo day E7.5 and the late crescent stage at E8.0, but was barely detectable in the linear heart tube after E8.5. In contrast, the expression of Noggin at the notochord continued after E8.5, as reported previously[7,8]. Sectioning of whole-mount samples from E7.5 and E8.0 showed expression of Noggin in both the endodermal and mesodermal layers and made clear that Noggin was derived from the primary heart field (**Fig. 1c,d**). This marked difference in the time course of Noggin expression between the heart-forming region and notochord suggested that transient expression of Noggin functions in cardiomyocyte differentiation.

We stimulated mouse ES cells in suspension cultures with Noggin in various ways (**Fig. 2a,b**). We administered Noggin before or after embryoid body formation to mimic the transient and strong expression of Noggin at the early gastrulation stage. Discontinuation of leukemia inhibitory factor (LIF) and addition of Noggin before or after embryoid body formation did not increase the incidence of formation of spontaneously beating embryoid bodies (**Fig. 2b**, rows 2,3). Interestingly, addition of Noggin on day 0 and discontinuation of LIF on day 3 slightly but substantially increased the beating embryoid body incidence (**Fig. 2b**, row 4), suggesting that the optimal timing for Noggin might be both before and after embryoid body formation. Next, we added Noggin at either −3, 0, +1, +2 or +3 d (**Fig. 2b**, rows 5–9), and LIF before embryoid body formation. Although Noggin at day 0 (**Fig. 2b**, row 6) slightly increased the beating embryoid body incidence, this incidence gradually decreased at the later time points. Based on these results, we administered Noggin at day −3 and day 0 from embryoid body formation. This led to a marked increase in beating embryoid body incidence to 95.3% at 10 d (**Fig. 2b**, rows 10–16), and continued growth of embryoid bodies to day 14. These results suggest that the cardiomyocyte inductive activity of Noggin was restricted to the period from 3 d before one day after embryoid body formation and that the ES cells must initially be undifferentiated.

This protocol was effective in two independent ES cell lines, EB3 and R1, and the optimal concentration of Noggin was 150 ng/ml (**Fig. 2c** and **Supplementary Fig. 1** online). To demonstrate that this effect was specific to inhibition of the BMP pathway, we administered various concentrations of BMP2 at day 0 (**Fig. 2d**). Even low doses of BMP2 strongly inhibited Noggin-dependent cardiomyocyte induction. To confirm that the inhibition of BMP signaling in the early

[1]Division of Cardiology, Department of Medicine, Keio University School of Medicine, 35 Shinanomachi, Shinjuku-ku, Tokyo 160-8582, Japan. [2]Department of Regenerative Medicine and Advanced Cardiac Therapeutics, Keio University School of Medicine, 35 Shinanomachi, Shinjuku-ku, Tokyo 160-8582, Japan. [3]Department of Physiology, Keio University School of Medicine, 35 Shinanomachi, Shinjuku-ku, Tokyo 160-8582, Japan. [4]Daiichi Suntory Biomedical Research Co. Ltd., 1-1-1 Wakayamadai, Shimamoto-cho, Mishima-gun, Osaka 618–8513, Japan. [5]Core Research for Evolutional Science and Technology (CREST), Japan Science and Technology Agency (JST), Kawaguchi, Saitama, 332-0012, Japan. Correspondence should be addressed to K.F. (kfukuda@sc.itc.keio.ac.jp).

Published online 1 May 2005; doi:10.1038/nbt1093

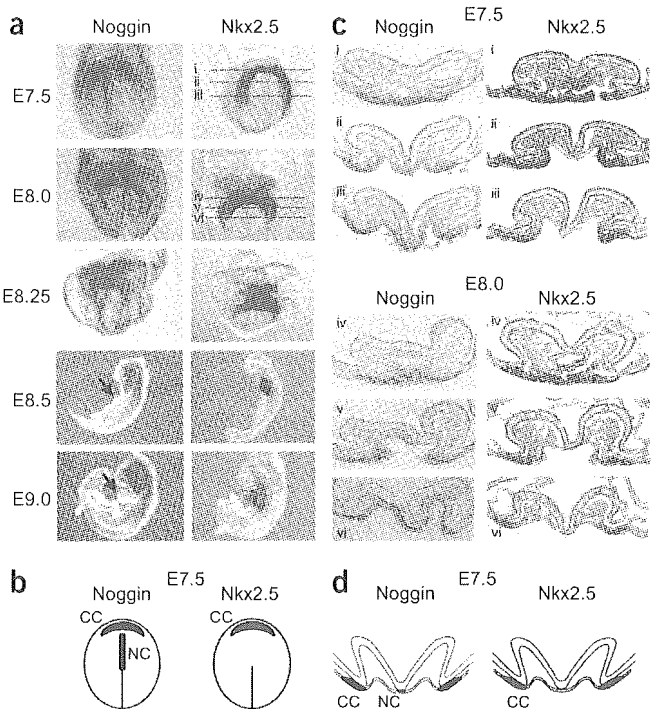

Figure 1 Transient expression of noggin at the heart forming area. (**a**) Whole-mount *in situ* hybridization of noggin and Nkx2.5 was performed at mouse embryo stages E7.5, E8.0, E8.25, E8.5 and E9.0. Note that noggin was strongly expressed at the cardiac crescent (E7.5) and late crescent stage (E8.0), but was undetected after E8.5. In contrast, Nkx2.5 was expressed thereafter. Arrows indicate the heart. (**b**) The schema of noggin and Nkx2.5 expression at E7.5. CC: cardiac crescent, NC: notochord, LHT: linear heart tube. (**c**) Section of samples at E7.5 and E8.0 with the whole mount *in situ* hybridization. i–vi represented the site of the section as shown in **a**. (**d**) The schema of noggin and Nkx2.5 expression at E7.5.

phase of differentiation could accelerate cardiomyocyte induction, soluble BMP receptor-1A (BMPR-1A) or another BMP antagonist, chordin, was also administered, and cardiomyocyte induction was observed. Both interventions augmented the incidence of beating in individual embryoid bodies (**Fig. 2e**). In contrast, administration of various growth factors, including insulin-like growth factor-1 (IGF-1), fibroblast growth factor (FGF2) and BMP2, using the same protocol did not boost cardiomyocyte induction (**Fig. 2f**). These results suggest that inhibition of BMP signaling in the undifferentiated or immediate early phase of ES cell differentiation is crucial for cardiomyocyte differentiation.

Next, we examined which step of cardiomyocyte development Noggin acted upon. Noggin-treated ES cells expressed markedly higher levels of brachyury T than untreated cells, and then showed strong induction of cardiomyocyte marker gene expression (Nkx2.5 and Tbx5). Despite this increase in brachyury-T expression, the expression of other early mesodermal markers transiently increased but then subsequently decreased (**Fig. 2g**). We also performed whole mount *in situ* hybridization of the embryoid bodies, and quantified these mesodermal marker-positive cells (**Fig. 2h,i**). Taken together, these data suggest that Noggin acts principally between the undifferentiated and brachyury-T-positive states. Brachyury T is a marker of mesendodermal progenitors that can differentiate into mesoderm or endoderm depending on culture conditions[9]. In our experiments, Noggin increased both the proportion of the cells expressing brachyury T by 1.8-fold and the level of brachyury-T mRNA per cell by sixfold (**Fig. 2j**). This suggests that an increase in mRNA per cell is essential for cardiomyocyte induction from undifferentiated ES cells, and that there may be subpopulations within the brachyury-T-positive cells that can be distinguished by their levels of expression. The increase in cells expressing high levels of brachyury T that formed mesendoderm resulted in the large increase in Nkx2.5-positive cells.

To quantify the incidence of cardiomyocyte induction with Noggin treatment, we immunostained for cardiac-specific proteins and observed the results by confocal laser microscopy. Most cells in the Noggin-treated embryoid bodies stained positive for myosin heavy chain (MHC), myosin light chain (MLC), atrial natriuretic peptide (ANP), cardiac troponin I and sarcomeric actinin (**Fig. 3a–c**). In contrast, the cardiomyocyte content was markedly lower in the control or in embryoid bodies treated with other Noggin protocols. The optimal Noggin protocol led to synchronous beating of the entire embryoid body (see **Supplementary Video** online). The isolated cells expressed many cardiac markers and had a typical cardiac myocyte morphology. At day 10, the embryoid bodies were attached to the gelatin-coated dishes and stained with anti-MHC antibodies. There was an ~100-fold increase in the number of cardiomyocytes compared with control.

The Noggin protocol efficiently induced expression of cardiac transcription factors, including Nkx2.5, GATA4, TEF1, Tbx5 and MEF2C, whereas expression of the stem cell marker Oct3/4 rapidly decreased (**Fig. 3d**). Cardiac-specific proteins were also strongly induced, including ANP, brain natriuretic peptide, MLC-2v, MLC-2a, α-MHC, β-MHC and α-cardiac actin. Western blot analysis revealed that the Noggin-treated embryoid bodies expressed GATA4, troponin I, MLC and ANP at levels that were 10- to 450-fold higher than those seen with the other protocol (**Fig. 3e,f**). To investigate whether this inductive phenomenon was cell autonomous or non-autonomous, we treated ES cells stably transfected with the gene encoding green fluorescent protein (GFP) with Noggin, and then combined them with untreated GFP^- ES cells just before embryoid body formation. The majority of GFP^+, Noggin-treated ES cells differentiated into cardiomyocytes in the embryoid bodies, whereas very few GFP^- untreated ES cells became cardiomyocytes (**Fig. 3g,h**). These findings suggest that Noggin-mediated induction of cardiomyocyte formation is a cell-autonomous phenomenon.

A number of growth factors and chemical compounds induce cardiomyocyte differentiation of mouse ES cells, including reactive oxygen species (2.7-fold increase in beating embryoid body incidence)[10], TGFβ plus BMP2 (threefold increase)[11], targeting of RBP-Jκ (downstream of notch signaling)-gene (20-fold increase)[12], ascorbic acid (fivefold increase)[13], as well as IGF-1, FGF, oxytocin, erythropoietin, retinoic acid and dimethyl sulfoxide[14–16]. To our knowledge, however, no previous protocol for increasing cardiomyocyte differentiation is as efficient as our present protocol (approximately 100-fold increase in the number of cardiomyocytes compared with control). The efficiency of our protocol may reflect the fact that it makes use of endogenous factors and is modeled on *in vivo* cardiomyoctye induction.

Accumulating evidence implicates BMP signaling as a potent heart-inductive signal. Administration of BMP-2/BMP-4 to explant cultures from chicken embryo induces full cardiac differentiation in stages 5–7 anterior medial mesoderm, a tissue that is normally not cardiogenic[17,18]. In contrast, before stage 3 or during early stages of gastrulation, both BMP2 and BMP4 inhibit cardiomyogenesis[19].

Although BMPs are expressed in lateral plate mesoderm including the anterior lateral plate[20], stimulation of ES cells by BMP2 or BMP4 does not augment cardiomyocyte differentiation. Together, these findings suggest that BMPs play multiple roles in mesodermal induction and specific organ differentiation and that their temporal and spatial expression is critical in cardiomyocyte induction[19].

In the vertebrate nervous system, the local action of Noggin and other BMP inhibitors on BMP signaling is very important in neural induction, in patterning during embryonic development and in adult neurogenesis[21]. In *Xenopus laevis* gastrula-stage embryos, Noggin and other BMP inhibitors are secreted by the Spemann organizer and induce neural tissue from dorsal ectoderm[7,22,23] by inhibiting ectodermal BMPs[24]. In the developing neural tubes, BMP has been shown to specify the dorsal fates of neural progenitor cells[25]. BMP inhibitors are also expressed in ventral somites or in the notochord, suggesting that some are involved in a counter gradient of BMP activity along the dorso-ventral axis.

Based on the analogy to the central nervous system, we suspected that the context-dependent differential action of BMPs in cardiomyocyte induction might be explained by local action of Noggin and other BMP inhibitors. We found that Noggin is transiently but strongly expressed at the anterolateral plate in mouse embryos at E7.0–E8.0 and is critical in cardiomyocyte induction. The restricted and highly effective window of Noggin's inductive action for cardiomyocyte differentiation from ES cells exactly matched the normal developmental conditions in the heart-forming area in E7.0-E8.0 embryos. From the present results, we propose that BMP signaling is essential for at least two steps in the cardiomyocyte induction

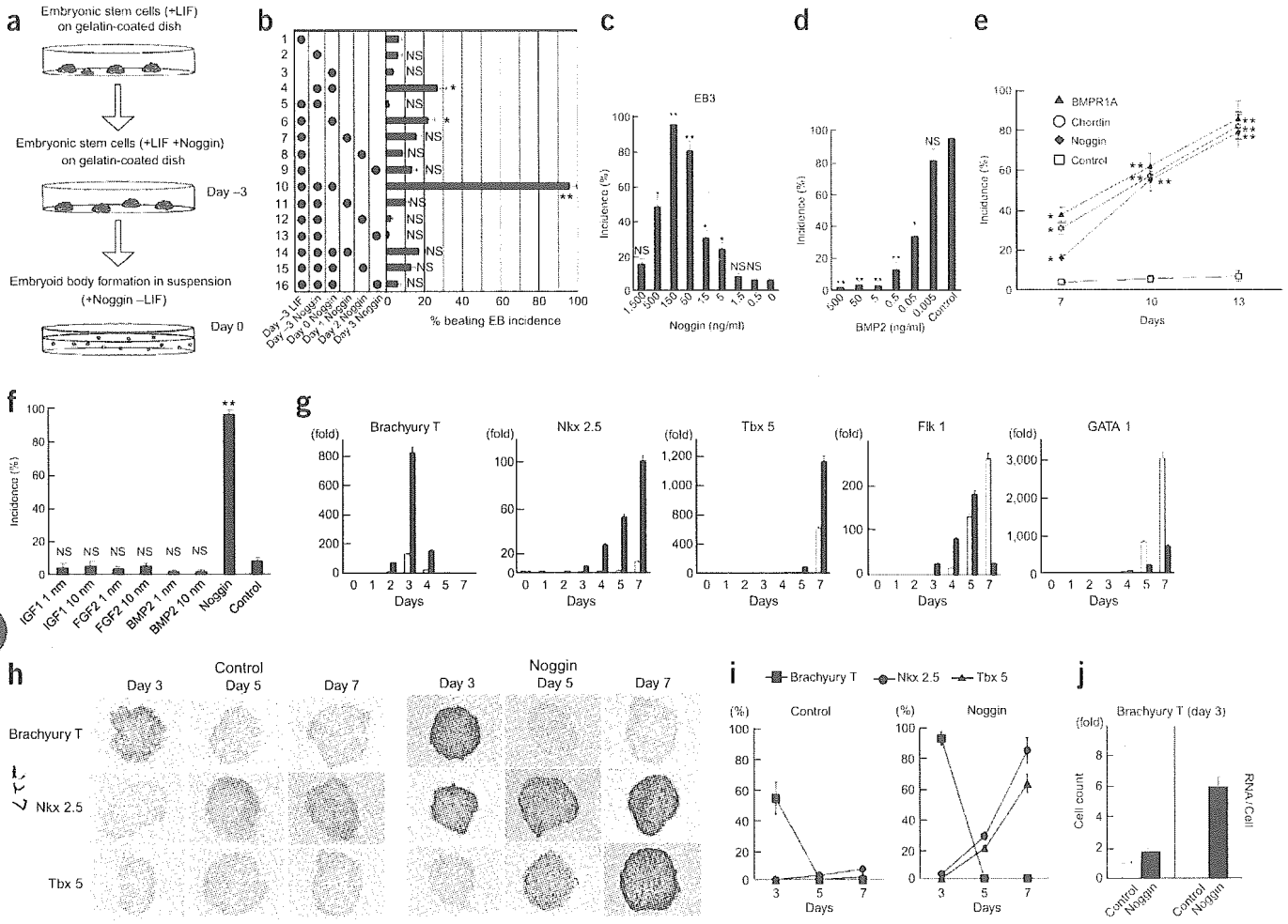

Figure 2 Protocol and efficiency of the cardiomyocyte induction from ES cells using noggin, chordin and soluble BMP receptor-1A. (**a**) Representative schema of the protocol of cardiomyocyte induction from ES cells. (**b**) The efficiency of various protocols for noggin (150 ng/ml) exposure were compared. (**c**) Dose-efficiency relationship of noggin administration was demonstrated using two different ES cell lines, EB3 and R1 (**Supplementary Fig. 1** online). Both lines showed the same dose-efficiency relationship. (**d**) Administration of low dose of BMP2 abolished the effect of noggin for cardiomyocyte induction, indicating the BMP2 concentration was critical in this phenomenon. (**e**) Effect of other BMP antagonists, chordin and soluble BMPR-1A (BMP neutralizing receptor), on cardiomyocyte induction. Both chordin and BMPR-1A were administered using the same protocol as noggin (150 ng/ml). Both of these BMP antagonists induced cardiomyocyte induction from ES cells at the same level as noggin, indicating that transient relief from the intrinsic BMP signal is critical for cardiomyocyte induction. (**f**) Other factors including IGF-1, FGF-2 and BMP2 did not affect cardiomyocyte induction with this protocol. (**g**) Quantitative RT-PCR of early mesodermal markers and cardiac transcription factors. Black column, noggin-treated ES cells; white column, nontreated ES cells. Each column was normalized by GAPDH. (**h**) Section of embryoid bodies at 3, 5 and 7 d after embryoid body formation with the whole mount *in situ* hybridization. (**i**) To identify individual cells in embryoid body sections, nuclei were stained with propidium iodide. Cells positive for brachyury T, Nkx2.5 and Tbx5 were counted. Cell numbers are presented as a percentage of the total. (**j**) The increased number of brachyury-T-positive cells and the increased levels of brachyury-T mRNA at day 3 after embryoid body formation are shown. $*P < 0.05$, $**P < 0.01$ versus control; NS, not significant.

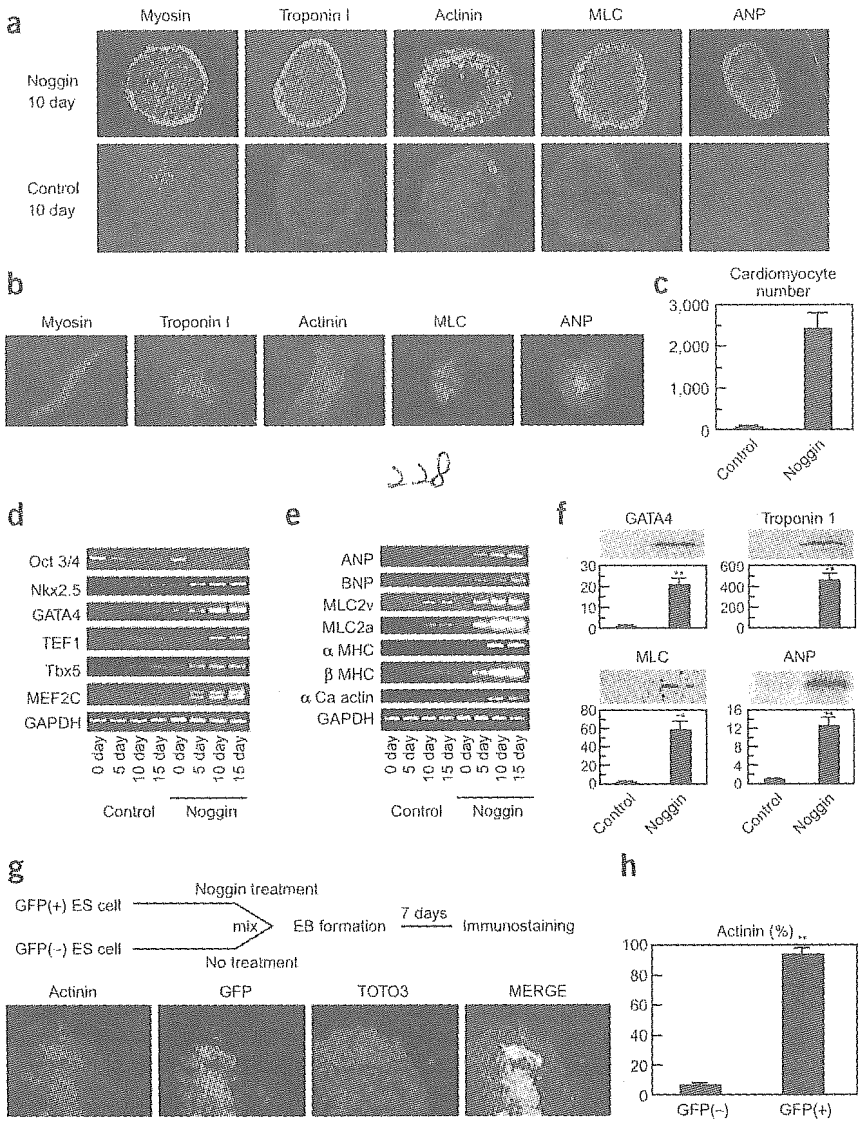

Figure 3 Expression of stem cell marker, cardiac transcription factors and cardiac specific proteins in noggin-treated ES cells. (**a**) Immunostaining for anti-MHC, anti-troponin I, anti-ANP, anti-actinin and anti-MLC are shown. Most of the cells in the whole embryoid bodies were stained with cardiomyocyte-specific antibodies. (**b**) Isolated cells were stained with the same antibodies. Red represents nuclear staining with PI. In the last immunofluorescent photograph, ANP, MHC and nucleolus are stained with rhodamine, FITC and DAPI, respectively. (**c**) Embryoid bodies were attached to the gelatin-coated tissue culture plate, and stained with anti-MHC and examined for the number of cardiomyocytes. The number of cardiomyocytes with noggin-treated cells was 100-fold more than the control cells. $^{**}P < 0.01$ versus control. (**d**) RT-PCR of Oct3/4, and cardiac transcription factors including Nkx2.5, GATA4, TEF1, Tbx5 and MEF2C is shown. Noggin treatment facilitated the extinction of Oct3/4 and accelerated the time and degree of cardiac transcription factor expression. (**e**) RT-PCR of cardiac-specific proteins. Noggin treatment augmented their expression. (**f**) Western blot analysis of cardiac-specific proteins. $^{**}P < 0.01$ versus control. (**g**) Cell autonomy of the noggin-treated ES cells. GFP^+ ES cells were treated with noggin, mixed with untreated GFP^- ES cells and embryoid body formation was performed. GFP^+ cells expressed actinin, whereas GFP^- cells did not. (**h**) Quantitative analysis of **g**. ANP, atrial natriuretic peptide; MLC, myosin light chain; BMP, bone morphogenetic protein; MHC, myosin heavy chain; GFP, green fluorescent protein; BNP (brain natriuretic peptide).

process: mesodermal induction[26] and cardiomyocyte differentiation[1,2]. However, between these steps, a transient block of intrinsic BMP signaling may be the most important step for determining cardiomyogenic differentiation.

METHODS

Whole-mount *in situ* hybridization. Pregnant ICR wild-type mice were purchased from Japan CLEA. All experiments were approved by the Keio University Ethics Committee for Animal Experiments. Mice from embryonic day (E) 7.5, 8.0, 8.25, 8.5 and 9.0 were removed, and whole-mount *in situ* hybridization was performed using digoxigenin-labeled RNA probes as described[27]. The full-length cDNAs for mouse *Noggin* and *nkx2.5* (accession number NM_008711 and NM_008700, respectively) were obtained by RT-PCR and subcloned into pBluescript plasmid. The cDNAs for mouse Tbx5 and brachyury T were kindly provided by H. Yamagishi and H. Bernhard, respectively. The probes were transcribed with T3 or T7 RNA polymerase.

Cell culture. Mouse embryonic fibroblast-free ES cells were used. Undifferentiated ES cells (EB3[28], R1[29]) were maintained on gelatin-coated dishes in GMEM supplemented with 10% FBS (Equitechbio), 2 mM L-glutamine, 0.1 mM nonessential amino acids, 1 mM sodium pyruvate, 0.1 mM 2-mercaptoethanol and 2,000 U/ml murine LIF (Chemicon International). EB3 cells (a kind gift from H. Niwa, Riken, Japan), which carry the blasticidin S-resistant selection marker gene driven by the Oct3/4 promoter (active in the undifferentiated status) were maintained in medium containing 20 μg/ml blasticidin S to eliminate differentiated cells. EB3 is a subline derived from E14tg2a ES cells[30], and was generated by targeted integration of the Oct3/4-IRES-BSD-pA vector[28] into the Oct3/4 allele.

Differentiation of ES cells. ES cells were cultured on gelatin-coated dishes in α-MEM supplemented with 10% FBS (Equitechbio), 2 mM L-glutamine, 0.1 mM nonessential amino acids, 1 mM sodium pyruvate, 0.1 mM 2-mercaptoethanol, 2,000 U/ml LIF and 0.15 μg/ml Noggin (Noggin-Fc, R&D) for 3 d. Then, the cells were trypsinized, and cultured to form spheroids (embryoid bodies) from a single cell using a three-dimensional culture system in the same medium as described above minus the LIF on uncoated Petri dishes to induce embryoid bodies. FGF2, IGF-1, BMP2, chordin and BMP receptor-1A/Fc (BMPR-1A) were purchased from R&D.

Histological and immunohistochemical analysis. Embryoid bodies (12–14 d) were fixed in 4% paraformaldehyde for 45 min and embedded using Tissue-Tek OCT (Sakura Finetek). In some experiments, the isolated cells were plated on gelatin-coated glass coverslips at low density and fixed in 4% paraformaldehyde for 5 min. The samples were exposed to primary antibodies including anti-MHC (MF20), anti-troponin I (C-19, Santa Cruz

Biotechnology; 1:500), anti-actinin (EA-53, Sigma; 1:800), anti-ANP (CHEMICON; 1:100), and anti-MLC (P-18, Santa Cruz; 1:500). Bound antibodies were visualized using a secondary antibody conjugated with Alexa488. Nuclei were stained with 4′,6-diamidine-2-phenylidole dihydrochloride (DAPI; Sigma Aldrich) or propidium iodide (PI, Sigma), TOTO3 (Molecular Probes). The percentage of MHC–expressing cells was quantified using the day-12 embryoid bodies.

RT-PCR and real-time quantitative PCR. Total RNA was extracted using Trizol reagent (GIBCO) and RT-PCR was performed as described previously[28]. At least five replicates were done for each time point. The PCR primers are listed in the **Supplementary Table 1** online. Before quantitative analysis, the linear range of the PCR cycles was measured for each gene, and the appropriate number of PCR cycles was determined. GAPDH was used as an internal control. For quantitative analysis of brachyury T, Nkx2.5, Tbx5, Flk1 and GATA1 expression, cDNA was used as template in a TaqMan real-time PCR assay using the ABI Prism 7700 sequence detection system (Applied Biosystems) according to the manufacturer's instructions. All samples were run in triplicate. Data were normalized to GAPDH. The primers and TaqMan probe for brachyury T, Nkx2.5, Tbx5, Flk1 and GATA1 were Mm00436877_m1, Mm00657783_m1, Mm00803521_m1, Mm00440099_m1, and Mm00484678_m1 (Applied Biosystems), respectively.

Western blotting. Embryoid bodies were lysed in a buffer containing 20 mmol/l Tris-HCl (pH 7.4), 100 mmol/l NaCl, 5 mmol/l EDTA, 1.0% Triton X-100, 10% glycerol, 0.1% SDS, 1.0% deoxycholic acid, 50 mmol/l NaF, 10 mmol/l $Na_3P_2O_7$, 1 mmol/l Na_3VO_4, 1 mmol/l phenylmethylsulfonyl fluoride, 10 μg/ml aprotinin, and 10 μg/ml leupeptin. Proteins were separated on 5% to 10% SDS-PAGE. Western blot analysis was performed as described previously[29]. Rabbit polyclonal antibodies against GATA4 (Santa Cruz Biotechnology), troponin I, MLC and ANP were used as primary antibodies, and peroxidase-conjugated goat anti-rabbit IgG was used as a secondary antibody. Signals were visualized with an ECL kit (Amersham).

Statistical analysis. The data were processed using StatView J-4.5 software. Values are reported as means ± s.d. Comparisons among values for all groups were performed by one-way ANOVA. The Scheffe's F test was used to determine the level of significance. The probability level accepted for significance was $P < 0.05$.

Note: Supplementary information is available on the Nature Biotechnology website.

ACKNOWLEDGMENTS

This work was (partially) supported by a grant-in-aid from the 21st century Center of Excellence Program of the Ministry of Education, Culture, Sports, Science and Technology, Japan to Keio University. We are grateful to H. Niwa for kindly providing ES cell line EB3 and T. Yoshizaki and Y. Okada for their thoughtful advice and discussion.

COMPETING INTERESTS STATEMENT

The authors declare that they have no competing financial interests.

Received 21 September 2004; accepted 30 March 2005
Published online at http://www.nature.com/naturebiotechnology/

1. Winnier, G., Blessing, M., Labosky, P.A. & Hogan, B.L. Bone morphogenetic protein-4 is required for mesoderm formation and patterning in the mouse. *Genes Dev.* **9**, 2105–2116 (1995).
2. Zhang, H. & Bradley, A. Mice deficient for BMP2 are nonviable and have defects in amnion/chorion and cardiac development. *Development* **122**, 2977–2986 (1996).
3. Marvin, M.J., Di Rocco, G., Gardiner, A., Bush, S.M. & Lassar, A.B. Inhibition of Wnt activity induces heart formation from posterior mesoderm. *Genes Dev.* **15**, 316–327 (2001).
4. Mima, T., Ueno, H., Fischman, D.A., Williams, L.T. & Mikawa, T. Fibroblast growth factor receptor is required for *in vivo* cardiac myocyte proliferation at early embryonic stages of heart development. *Proc. Natl. Acad. Sci. USA* **92**, 467–471 (1995).
5. Sasai, Y., Lu, B., Steinbeisser, H. & De Robertis, E.M. Regulation of neural induction by the Chd and Bmp-4 antagonistic patterning signals in *Xenopus*. *Nature* **376**, 333–336 (1995).
6. Lim, D.A. *et al.* A. Noggin antagonizes BMP signaling to create a niche for adult neurogenesis. *Neuron* **28**, 713–726 (2000).
7. Smith, W.C. & Harland, R.M. Expression cloning of noggin, a new dorsalizing factor localized to the Spemann organizer in *Xenopus* embryos. *Cell* **70**, 829–840 (1992).
8. McMahon, J.A. *et al.* Noggin-mediated antagonism of BMP signaling is required for growth and patterning of the neural tube and somite. *Genes Dev.* **12**, 1438–1452 (1998).
9. Kubo, A. *et al.* Development of definitive endoderm from embryonic stem cells in culture. *Development* **131**, 1651–1662 (2004).
10. Sauer, H., Rahimi, G., Hescheler, J. & Wartenberg, M. Role of reactive oxygen species and phosphatidylinositol 3-kinase in cardiomyocyte differentiation of embryonic stem cells. *FEBS Lett.* **476**, 218–223 (2000).
11. Behfar, A. *et al.* Stem cell differentiation requires a paracrine pathway in the heart. *FASEB J.* **16**, 1558–1566 (2002).
12. Schroeder, T. *et al.* Recombination signal sequence-binding protein Jkappa alters mesodermal cell fate decisions by suppressing cardiomyogenesis. *Proc. Natl. Acad. Sci. USA* **100**, 4018–4023 (2003).
13. Takahashi, T. *et al.* Ascorbic acid enhances differentiation of embryonic stem cells into cardiac myocytes. *Circulation* **107**, 1912–1916 (2003).
14. Boheler, K.R. *et al.* Differentiation of pluripotent embryonic stem cells into cardiomyocytes. *Circ. Res.* **91**, 189–201 (2002).
15. Heng, B.C., Haider, H.K., Sim, E.K., Cao, T. & Ng, S.C. Strategies for directing the differentiation of stem cells into the cardiomyogenic lineage *in vitro*. *Cardiovasc. Res.* **62**, 34–42 (2004).
16. Sachinidis, A. *et al.* Cardiac specific differentiation of mouse embryonic stem cells. *Cardiovasc. Res.* **58**, 278–291 (2003).
17. Schultheiss, T.M., Burch, J.B. & Lassar, A.B. A role for bone morphogenetic proteins in the induction of cardiac myogenesis. *Genes Dev.* **11**, 451–462 (1997).
18. Andree, B., Duprez, D., Vorbusch, B., Arnold, H.H. & Brand, T. BMP-2 induces ectopic expression of cardiac lineage markers and interferes with somite formation in chicken embryos. *Mech. Dev.* **70**, 119–131 (1998).
19. Ladd, A.N., Yatskievych, T.A. & Antin, P.B. Regulation of avian cardiac myogenesis by activin/TGFbeta and bone morphogenetic proteins. *Dev. Biol.* **204**, 407–419 (1998).
20. Lyons, K.M., Hogan, B.L. & Robertson, E.J. Colocalization of BMP 7 and BMP 2 RNAs suggests that these factors cooperatively mediate tissue interactions during murine development. *Mech. Dev.* **50**, 71–83 (1995).
21. Lim, D.A. *et al.* Noggin antagonizes BMP signaling to create a niche for adult neurogenesis. *Neuron* **28**, 713–726 (2000).
22. Smith, W.C., Knecht, A.K., Wu, M. & Harland, R.M. Secreted noggin protein mimics the Spemann organizer in dorsalizing *Xenopus* mesoderm. *Nature* **361**, 547–549 (1993).
23. Lamb, T.M. *et al.* Neural induction by the secreted polypeptide noggin. *Science* **262**, 713–718 (1993).
24. Zimmerman, L.B., De Jesus-Escobar, J.M. & Harland, R.M. The Spemann organizer signal noggin binds and inactivates bone morphogenetic protein 4. *Cell* **86**, 599–606 (1996).
25. Liem, K.F. Jr., Jessell, T.M. & Briscoe, J. Regulation of the neural patterning activity of sonic hedgehog by secreted BMP inhibitors expressed by notochord and somites. *Development* **127**, 4855–4866 (2000).
26. Winnier, G., Blessing, M., Labosky, P.A. & Hogan, B.L. Bone morphogenetic protein-4 is required for mesoderm formation and patterning in the mouse. *Genes Dev.* **9**, 2105–2116 (1995).
27. Sasaki, H. & Hogan, B.L. Differential expression of multiple fork head related genes during gastrulation and axial pattern formation in the mouse embryo. *Development* **118**, 47–59 (1993).
28. Niwa, H., Miyazaki, J. & Smith, A.G. Quantitative expression of Oct-3/4 defines differentiation, dedifferentiation or self-renewal of ES cells. *Nat. Genet.* **24**, 372–376 (2000).
29. Nagy, A., Rossant, J., Nagy, R., Abramow-Newerly, W. & Roder, J.C. Derivation of completely cell culture-derived mice from early-passage embryonic stem cells. *Proc. Natl. Acad. Sci. USA* **90**, 8424–8428 (1993).
30. Hooper, M., Hardy, K., Handyside, A., Hunter, S. & Monk, M. HPRT-deficient (Lesch-Nyhan) mouse embryos derived from germline colonization by cultured cells. *Nature* **326**, 292–295 (1987).

心室 remodeling と HCM/DCM の狭間

順天堂大学医学部循環器内科

河合祥雄、鈴木宏昌、山田京志、代田浩之

抄録

【背景】拡張型心筋症は内腔拡張、収縮力の低下を、肥大型心筋症は壁肥厚、収縮力低下のないことを前提とする。肥大型心筋症と拡張型心筋症とは独立した病態と理解されてきたが、拡張相肥大型心筋症、拡張型心筋症の reverse remodeling の概念は、拡張型心筋症、肥大型心筋症のいずれでもない形態（中間型もしくは型不明型心筋症）が存在することを前提とする。

【目的】型不明型心筋症の相対的位置付けを、中間型心筋症の拡張、肥厚の偏位ベクトルおよび病理形態から検討する。

【方法】心筋症の左室形態は、心エコー図計測値の壁肥厚(>12mm)、左室拡張期内径拡大（>55mm)、収縮低下の有無で８型に分類できる。+/-で表すと、正常は[- - -]、肥大型心筋症は[+ - -]、拡張型心筋症は[- + +]。残りの５型は肥大型心筋症、拡張型心筋症のいずれでもない型不明型心筋症（中間型）となる。心筋症連続心筋生検 1,388 例より、拘束型心筋症、不整脈源性右室異形成症、特定心筋疾患を除外した 471 症例における中間型の経時的な左室形態の変化、組織所見などを検討した。

【結果】肥大型心筋症 240、拡張型心筋症 120、中間型 111 例。経過追跡した 61 例中、拡張例 14（肥大型→中間型:3、中間型→拡張型:10、肥大型→中間型→拡張相肥大型心筋症:1）、肥厚例 13（拡張相肥大型心筋症→中間型:5、中間型→肥大型:8）が存在した。高度錯綜配列、ミトコンドリア心筋症類似の空胞変性、心疾患家族歴は、それぞれ 14:15:6%、14:31:19%、29:15:13%に存在した。

【総括】典型的肥大型心筋症と拡張型心筋症との狭間にある型不明型心筋症は、狭義の心筋症の約 1/4 を占め、拡張相肥大型心筋症の途中経過のみならず肥大型心筋症に伸展する例も含む、多様な形態を示した。空胞変性の頻度が高く、単なる肥大型心筋症からの移行例、いわゆる reverse remodeling でない可能性がある。

従来、肥大型心筋症（HCM）と拡張型心筋症（DCM）とは独立した病態と理解されてきたが、拡張相肥大型心筋症（d-HCM）、DCMのreverse remodelingの存在は、典型的DCM、典型的HCMのいずれでもない形態（中間型もしくは型不明型心筋症）を認めることを意味する。現行分類ではHCM, DCM, 拘束型心筋症、不整脈原性右室心筋症のいずれにも分類されない症例はunclassified cardiomyopathy（型不明型心筋症）に分類される[1]が、その内容は明確ではなく、ましてそれらを検討した報告は少ない[2]。HCM、DCM共に明確な数値基準がないことも相まって、実際の心筋症症例はHCM、DCMいずれかの病型と診断するバイアスが存在する。

目的

一定の数値的基準をおいて、HCM、DCMを分類した場合に生じうる、分類不能例の頻度、その臨床的特徴を明らかにする作業に加えて、この中間型心筋症群の偏位ベクトル（拡張、肥厚）および病理形態を、生検症例を用いて検討した。

対象と方法

当科で検鏡した心筋疾患連続生検1,388例のうち拘束型心筋症、不整脈原性右室心筋症、不整脈を主徴とする心筋疾患[3]、心筋炎を含む特定心筋疾患を除外した症例を対象とした。アルコール長期多飲歴が認められ、かつ、心筋生検にて病理組織学的に、心筋細胞内のPAS陽性顆粒や脂肪滴、間質の脂肪細胞や細胞周囲性の淡い線維症などの所見が得られたものは、アルコール性心筋疾患[4]として特定心筋疾患に分類した。心筋炎は先行する感冒症状および心筋炎に由来すると考えうる他覚的所見を有するか、または心筋組織にて心筋炎と考えられる組織所見[5、6]を呈したものとした。

分類

対象を、拘束型心筋症で用いられた数値基準(左心室駆出率≧50%、左心室拡張終期径≦55mm、 または左心室拡張終期容量≦150ml、 心室中隔壁厚≦12mm、 左心室厚壁壁厚≦12mm、左心室拡張終期圧>12mmHg)を準用し、心エコー図よりの計測値：A.壁肥厚［心室中隔厚＞12mm または左室後壁厚＞12mm］、B.左室拡張末期径拡大［左室拡張末期径＞55mm］、C. 収縮能低下［左室駆出率＜50%］の有無で分類した。

各パラメーターを+/-で表記すると（［A B C］）、収縮能は左室拡張末期径と左室収縮末期径から求められるのであるから、それぞれは独立であり、症例は８型 （

[- - -]、[- - +]、[- + -]、[- + +]、[+ - -]、[+ - +]、[+ + -]、[+ + +])
に分けることができる。この記載法を用いると正常心は [- - -]、HCM は [+ - -]、DCM は [- + +] と表され、従って残りの [- - +]、[- + -]、[+ - +]、[+ + -]、[+ + +] は特発性心筋症の四大型に属さない型不明型心筋症となる（図１）。

図１　Classification of Cardiomyopathies

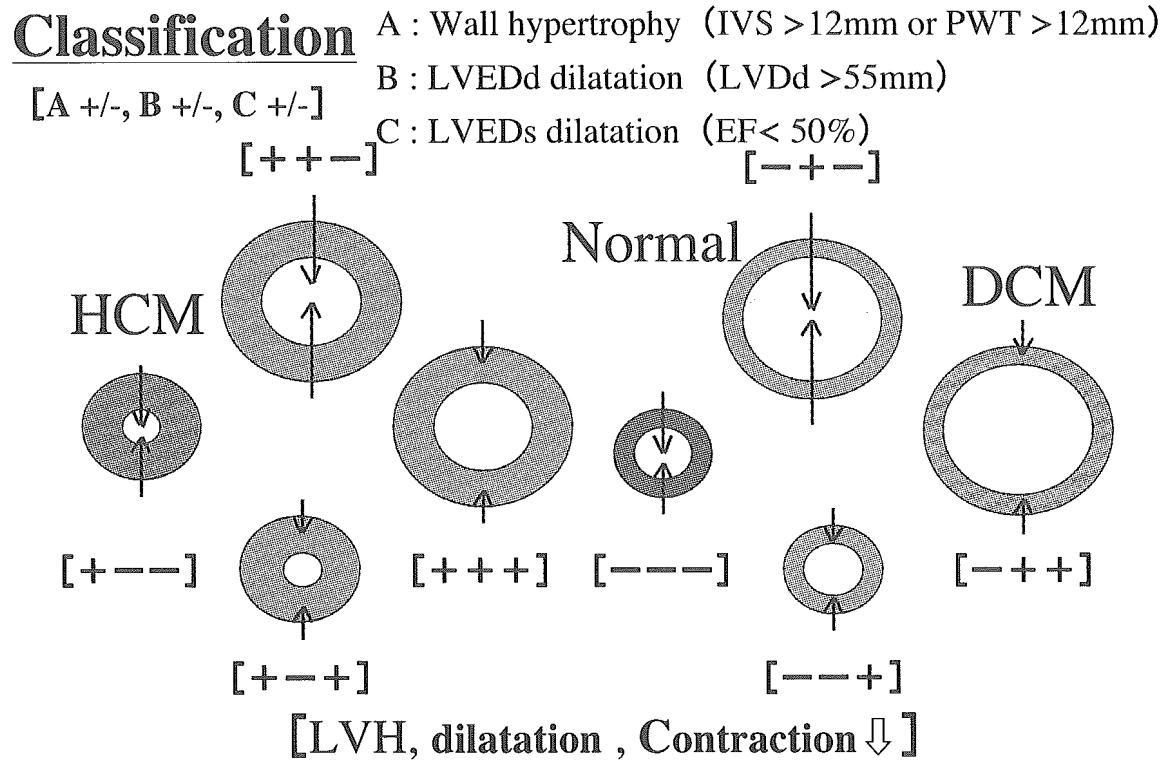

The patients with idiopathic cardiomyopathies were classified into eight subgroups on the basis of the echocardiographic measurements. i.e. Presence or absence of the following three parameters; A. left ventricular hypertrophy (septal or posterior wall thickness＞12mm), B. left ventricular dilatation (left ventricular diastolic dimension＞55mm), C. systolic dysfunction (left ventricular ejection fraction＜50%) is signified by plus or minus ([A B C]). HCM, DCM and normal heart are signified as [+ - -] , [- + +] and [- - -] , respectively. Therefore, unclassified cardiomyopathy (UCM) are signified as either [+ + -] , [+ - +] , [+ + +] , [- + -] or [- - +] .

家族歴

心筋症、突然死を含む心疾患家族歴の有無を病歴または主治医を通じて調査した。

組織所見

心筋生検標本所見より、組織学的に心筋細胞肥大、変性、錯綜配列、線維症の程

度を0～3+の４段階に分類した。3+を高度とし、高度変性、高度錯綜配列、高度線維症の頻度を型別に求め、HCM、DCM、型不明型心筋症間でχ2-testを用いて比較検討した。

経過追跡

型不明型心筋症全例を、病歴または主治医を通じて左室形態がどの型からどの型へ移行したかを追跡した。

経過中、左室内腔が拡張（左室拡張末期径＞55mm）したもの、逆に内腔拡張が消失した（左室拡張末期径≦55mm）症例の病理組織所見を検討した。

結果

心筋症関連心筋生検例は1,388例で、HCM 240例（17.3%）、平均年齢50 +/- 15 歳（女性:50人）、DCM 120例（8.6%）、平均年齢50 +/- 14 歳（女性:30人）、拘束型心筋症 11例（0.8%）、不整脈原性右室心筋症20例（1.4%）、不整脈を主徴とする心筋疾患 104例（7.5%）、特定心筋疾患 782例（56.3%）、型不明型心筋症 111例（8.0%）、平均年齢51 +/- 13 歳（女性:20人）よりなる。分析にはHCM、DCM、型不明型心筋症の計471例を対象とした。

家族歴

HCM、DCM、型不明型心筋症各群の心疾患家族歴の頻度は29%、15%、13%でHCMと型不明型心筋症との間で有意差を認めるものの($p<0.01$)、DCMと型不明型心筋症との間で有意差を認めなかった。

組織所見

HCM、DCM、型不明型心筋症の各群間の高度錯綜配列頻度は、それぞれ14%、6%、15%で、HCMと型不明型心筋症との間で有意差を認めないものの、DCMと型不明型心筋症との間で有意差を認めた（$p<0.05$）。有意な変性の頻度はそれぞれ、８％、８％、８％、繊維症の頻度は８％、13%、11%であった。

空胞変性の頻度は、それぞれ14%、31%、19%で、型不明型心筋症はHCM（$p<0.01$）DCM（$p<0.05$）に比べ、有意差に多い出現頻度を認めた（表１）。

Table 1

Clinicopathologic findings

	HCM	UCM	DCM
FH	69 (29%)**	17 (15%)	15 (13%)
Disarray	34 (14%)		17 (15%)
7 (6%)*			
Vacuole	34 (14%)	34 (31%)	23 (19%)*

Family history of heart diseases including cardiomyopathy and sudden death

Frequency of family histories, myocardial disarray and vaucular degeneration.
HCM = Hypertrophic cardiomyopathy ; DCM = Dilated cardiomyopathy.
UCM = Unclasified cardiomyopathy ( ) : %, n : Number, * *: p <0.01, * : p <0.05

病型の移行

経過の追跡し得た（平均 6.3 +/- 6 年間）型不明型心筋症は 111 例中 71 症例で、そのうちのデータが完備した 61 例について分析した。HCM、DCM、型不明型心筋症 3 群間の移行は Figure の如くであった。

拡張例は14例で、その内訳は肥大型→中間型:3例、中間型→拡張型:10例、肥大型→中間型→拡張相肥大型心筋症:1例であった。組織学的に肥大５例、錯綜配列2(8)例，変性2 (7)例が見られた。肥厚例は13例で、その内訳は、拡張相肥大型心筋症→中間型:5例、中間型→肥大型:8例であった。組織は肥大１例、錯綜配列:4(8)例、変性2 (6)例であった。

Fig. 2

考察

錯綜配列の位置づけ

d-HCMの典型例は、肥大相から拡張相への移行の確認に加えて、組織学的に広範な錯綜配列と高度線維症を特徴としている[7]。錯綜配列はHCMに特徴的と理解されている[1]が、今回の検討では、高度錯綜配列頻度はHCMで14%と比較的低値であった。この値は河村らの報告や[8]や、1978年に施行された本邦剖検例のアンケート調査における検討結果[9])と一致し、一般に想定されるよりHCMで高度錯綜配列のみられる頻度は高くないことを意味していよう。

逆に，DCMに見られた高度錯綜配列は従来の知見と矛盾した。それは、拡張型心筋症に混入している壁厚の薄くなった拡張相肥大型心筋症を見ている可能性に加えて、錯綜配列自体が肥大型心筋症に特異的でないこと、例えば、筋強直性ジストロフィーでは錯綜配列がみられる[10)、11)]、を反映している可能性がある。錯綜配列は、心室のリモデリング、特に内腔拡張、壁の伸展では心筋線維配列錯綜度が増すことは想定されないので[12)]、型不明型心筋症に見られた錯綜配列は、中間型に移行した際に出現したと考えるよりは、それ以前から存在したと考える方が合理的である。中間型にはd-HCMが含まれるが均一ではなく、壁厚、内腔、収縮能は様々であるので、移行する経路も多様性をもっていることが推定された。

病型間の移行

中間型の追跡調査において、HCMからの移行例が３例認められたことは中間型にd-HCMが含まれるとする前述の考察を裏付けるものである。しかし、DCMからの移行例が５例も存在したことは注目すべき事実と考えられる。また、逆に中間型からHCMへの移行は８例に認められ、中間型はHCMの初期像としても留意する必要がある。 型不明型心筋症のうち、潜在性拡張型心筋症[13)]は、[- - +] 群に相当する。この群には、経過中、典型的DCMに至るものと、典型的HCMに至るものものが混在し、従来、潜在性拡張型心筋症と捉えられていた症例の中には、d-HCMへの移行型やHCMの初期像が含まれている可能性がある。

HCMに見られる内腔拡張はleft ventricular chamber dilatation、left ventricular enlargement、relative cavity dilatationなどと表現され[14]、この表現からは必ずしも典型的DCMには至らないことが窺える。これら拡張した肥大心（[+ + +]群）および収縮能の低下した肥大心（[+ - +]群）は、厳密な数値基準で区切れば、HCMとDCMとの狭間にある中間型である。

空胞変性の意味

今回の検討では、中間型に有意に空砲変性が多いことが示された。この空胞変性は、ミトコンドリア心筋症[15][16]に見られる空胞変性(vacuolar dystrophy[16])に酷似し、二次的心筋症の混在[17]を示唆する。

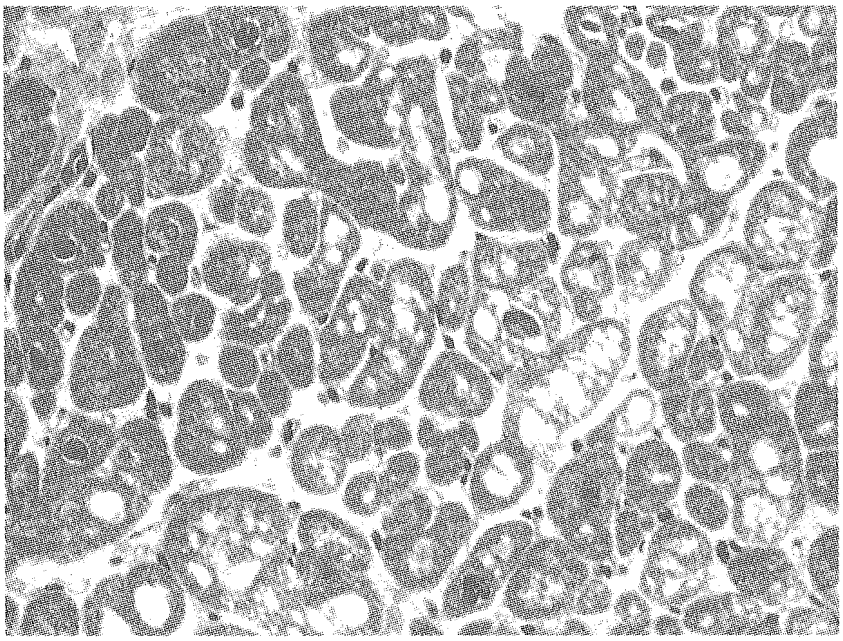

以上、中間型の検討からHCM、DCMは固定した病態ではなく、変化しうる一断面を捉えている可能性、ならびに中間型に特有の病理所見の存在が推察された。

謝辞

貴重な心筋生検症例の検索を御許可戴きました全国諸施設の先生方、および生検症例の追跡調査に御協力賜りました多くの諸先生に深謝致します。